ELSEVIER

Spin-resolved magnetic studies of focused ion beam etched nano-sized magnetic structures

Jian Li, Carl Rau *

*Department of Physics and Astronomy, Rice Quantum Institute and Center for Nanoscience and Technology,
Rice niversity, Houston, TX 77251, USA*

Abstract

Scanning ion microscopy with polarization analysis (SIMPA) is used to study the spin-resolved surface magnetic structure of nano-sized magnetic systems. SIMPA is utilized for in situ topographic and spin-resolved magnetic domain imaging as well as for focused ion beam (FIB) etching of desired structures in magnetic or non-magnetic systems. Ultra-thin Co films are deposited on surfaces of Si(100) substrates, and ultra-thin, tri-layered, bct Fe(100)/Mn/bct Fe(100) wedged magnetic structures are deposited on fcc Pd(100) substrates. SIMPA experiments clearly show that ion-induced electrons emitted from magnetic surfaces exhibit non-zero electron spin polarization (ESP), whereas electrons emitted from non-magnetic surfaces such as Si and Pd exhibit zero ESP, which can be used to calibrate sputtering rates in situ. We report on new, spin-resolved magnetic microstructures, such as magnetic "C" states and magnetic vortices, found at surfaces of FIB patterned magnetic elements. It is found that FIB milling has a negligible effect on surface magnetic domain and domain wall structures. It is demonstrated that SIMPA can evolve into an important and efficient tool to study magnetic domain, domain wall and other structures as well as to perform magnetic depth profiling of magnetic nano-systems to be used in ultra-high density magnetic recording and in magnetic sensors.
© 2004 Published by Elsevier B.V.

PACS: 75.60.Ch; 75.75.+a; 75.70.Rf; 81.16.Nd

Compared to continuous magnetic media, patterned, single- and multi-layered magnetic media are attracting more and more scientific and technological attention, because they not only allow to overcome fundamental thermal stability limits on data storage densities, but they are also expected to exhibit novel magnetic properties that contrast strikingly with the macroscopic properties of currently known materials. Presently, nano- and micron-sized, patterned magnetic elements are being explored for their practical use for ultra-high density magnetic storage (non-volatile, magnetic RAM), for miniaturized magnetic reading and writing heads, for magnetic sensor arrays and for

* Corresponding author. Tel.: +1 713 348 5417; fax: +1 713 348 4150.
  E-mail address: rau@rice.edu (C. Rau).

other nano-devices consisting of combinations of sensors, storage and processing units and spin transistors [1].

In recent years, focused ion beam (FIB) milling and etching, using Ga^+ ion beams for highly efficient fabrication of patterned nano- and micron-scale magnetic elements and arrays, including magnetic antidot arrays, has become a very promising experimental tool, both from a scientific and commercial point of view [2–6]. In these studies, the FIB milling or etching process is solely used to remove magnetic or non-magnetic material to fabricate patterned structures. The ion beam is not utilized for the irradiation of magnetic materials to study possible irradiation-dependent effects of the ion fluence on magnetic anisotropies and coercivities [7,8].

Central to the exploration of these new magnetic systems is the study of the mechanisms of magnetization reversal via the formation of distinct magnetic domain and domain wall structures and the study of a possible influence of the FIB milling process on the magnetic properties of FIB-created magnetic elements. Using FIB etching, the shape and size of patterned elements can easily be changed in situ, thereby allowing to study very efficiently the dependence of size and shape of patterned elements on magnetization reversal mechanisms. Understanding the reproducible reversal of the magnetization of single islands or elements of patterned magnetic systems, without disturbing neighboring elements, remains a great challenge in the fields of nano- and micromagnetism.

Note that non-uniform magnetization configurations in patterned structures play an important role in magnetization reversal processes [9,10]. Therefore, a deeper insight in the mechanisms of magnetization reversal can be obtained by applying in situ magnetic techniques that allow not only for a spin-resolved determination of the orientation and magnitude of the surface magnetization, but also for a determination of their surface topographic structure and their relation to the micromagnetic surface structure [6].

Using scanning ion microscopy with polarization analysis (SIMPA), we have already reported on the pinning of magnetic domains at surface defects that are directly visible in the topographical images obtained by using the SIMPA microscope [11]. Quite recently, we have shown that SIMPA can be applied to study micromagnetic configurations [6]. SIMPA has also been applied to study the interrelation between surface magnetic domain structures and magnetic couplings in tri-layered magnetic systems [12].

In SIMPA, a highly focused Ga^+ ion beam (minimum spot size: 35 nm) is scanned across a magnetic or non-magnetic surface of a sample thereby inducing the emission of spin polarized or non-spinpolarized electrons. The magnitude and orientation of the electron spin polarization (ESP) P of the ion-induced, emitted electrons is directly proportional to the magnitude and orientation of the magnetization existing at the local surface area from where the electrons are emitted. A magnetic image of the surface is obtained by rastering the ion beam across the magnetic surface [11]. SIMPA can be applied in situ to study micromagnetic configurations in great detail as well to fabricate in situ patterned magnetic elements and systems by using FIB milling.

In this paper, we present so-called spin-resolved configuration maps of the magnetization (spin maps) existing at surfaces of 20μm-sized, square-shaped and circular Co elements, which are created by FIB milling of 30 nm thin Co films deposited on Si(100) substrates. We further report on details of micromagnetic configurations of bct Fe(100)/fct Mn/bct Fe(100) sandwich structures deposited on fcc Pd(100) substrates. The various micromagnetic configurations are studied before, during and after FIB milling. It is found that the FIB milling process, used to remove magnetic material to create patterned magnetic elements, does not change the micromagnetic configurations existing at the surface of the tri-layered Fe/Mn/Fe film systems. We note that from these experiments, it is obvious that SIMPA can be developed into an efficient tool for magnetic sputter depth profiling.

30 nm Thick Co films are deposited on Si(100) substrates by using electron beam evaporation at a rate of 0.03 nm/s. For further experimental details, we refer to [6]. Next, 1–9 monolayer (ML) thin Mn wedges (deposition rate: 0.001 nm/s) are sandwiched between 35 ML thin bct Fe(100) and

50 ML thin bct Fe(100) films, which are deposited on clean and well characterized fcc Pd(100) substrates by using e-beam evaporation and a deposition rate of 0.002 nm/s. The pseudomorphic growth of the bct Fe and fct Mn films is monitored by using quantitative Auger electron spectroscopy (AES) and medium energy electron diffraction (MEED). No interdiffusion is found during the evaporation of the films. For further details, we refer to [12]. After preparation, all samples are studied by using the magneto-optical Kerr effect (MOKE).

For all Co films, perfectly square MOKE hysteresis loops with a coercivity field of 14.8 Oe are found. No change of size and shape of the square loops is observed upon rotation of the samples around the surface normal, indicating the presence of zero or randomly oriented magnetocrystalline anisotropy due to the very good polycrystalline nature of the Co films. For the Fe/Mn/Fe/Pd systems, MOKE experiments show square-shaped hysteresis loops and fourfold magnetic anisotropies along the easy axes, which are oriented along the $\langle 100 \rangle$ directions of the topmost bct Fe(100) films. No uniaxial magnetic anisotropies are found.

Subsequently, the samples are transferred from the MOKE chamber to the SIMPA microscope by using an UHV transfer manipulator. The SIMPA microscope is located in an UHV chamber operating at a base pressure in the low 10^{-10} mbar region. This chamber houses a scanning, microfocused 6–30 keV Ga^+ ion beam facility, which is used to scan magnetic and non-magnetic surfaces to induce the emission of electrons from the sample surface. By using an extraction lens systems and a spin-sensitive Mott detector, the orientation and magnitude of the electron spin polarization (ESP) P of the emitted electrons is analyzed in order to obtain spin-resolved images of magnetic domains, domain walls and other micromagnetic configurations. The SIMPA technique has some unique advantages over many other magnetic imaging techniques, because of its capability to produce vectorial maps of the surface magnetization by directly measuring the spatially resolved orientation and magnitude of the surface ESP. Mostly the two components of the in-plane

surface ESP are analyzed. However, the out-of-plane component can be obtained too by rotating the sample by 45°. For fast adjustment of imaging parameters and precise location of surface areas to be imaged, a conventional electron detector is used to display topographic images on a TV monitor at TV rates. For further details, we refer to [11,6,12].

FIB milling is used to fabricate patterned magnetic elements from 30 nm thin Co films deposited on Si (001) substrates. Fig. 1 shows a spin-resolved map of the surface magnetization obtained at the surface of an FIB created, square-shaped magnetic Co element (size: 20 μm). Before SIMPA imaging, the Co element is first created by FIB milling, then magnetized to saturation and subsequently brought to the remanent state. The black arrows represent the orientation and magnitude of the surface ESP, which is a characteristic of the surface magnetization. It is easily visible that the Co element is not uniformly magnetized. A so-called "C" shaped magnetization configuration is directly visible from the upper right and lower right part of the image. In order to obtain a clear
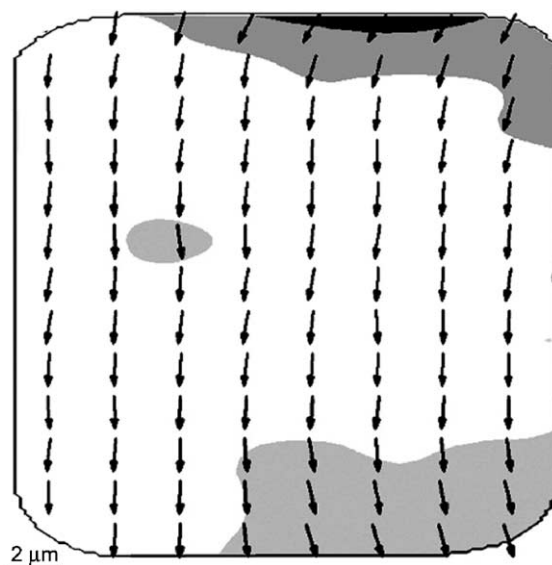

Fig. 1. SIMPA spin map of a square-shaped (size 20 μm), 30 nm thick Co/Si(100) element, fabricated by FIB milling and subsequently magnetized to saturation and then brought to the remanent state. A "C" shaped micromagnetic configuration can be identified from the distribution of the black arrows representing the local surface magnetization.

plot, the density of the black *P* vectors is reduced by a factor of 16, thereby making the "C" state more easily visible. The existence of such "C" states in small micromagnetic elements was theoretically predicted in 1997 by Zheng and Zhu [9].

Fig. 2 shows a spin configuration map obtained at the surface of a circular magnetic Co element (35 μm diameter) created by ion beam milling from a 30 nm thick Co/Si(1 0 0) film. The circular Co element is first created by ion beam etching, then brought to the demagnetized state and subsequently imaged by using SIMPA. The grey shades in the image represent different orientations of the in-plane ESP a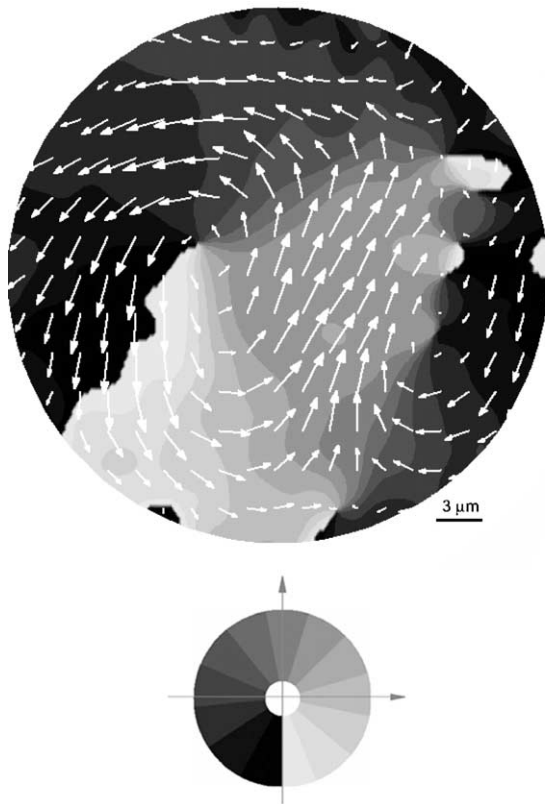s given by the grey shade wheel in the lower part of Fig. 2. The local orientation and magnitude of the *P* vectors is given by white arrows. The magnitude of *P* amounts to approximately 25%, which represents a 6% increase compared to the bulk magnetization of Co, which amounts to around 19%. The existence of such a surface enhanced magnetic order is theoretically expected. From the distribution of the *P* vectors it is clearly visible that the surface ESP is non-uniform. The curling of the *P* vectors shows the existence of magnetic vortex and anti-vortex states, which directly illustrates that such states have to be considered in realistic calculations or magnetic reversal mechanisms. We note that it was not possible to derive such vortex or anit-vortex states in magnetic simulations using the OOMMF code for micromagnetic calculations [13].

In order to be able to study possible influences of the FIB etching process on surface micromagnetic configurations, we have studied SIMPA spin maps before and after FIB milling. Fig. 3(a) shows the spin resolved magnetic domain image of a 270 μm × 400 μm size, wedge shaped bct Fe(1 0 0) (35 ML)/fct Mn/bct Fe(1 0 0) (50 ML)/fcc Pd (1 0 0) film, for a Mn spacer thickness of $d_{Mn} = 4$ ML, before FIB milling. The use of a wedged Fe/Mn/Fe/Pd film system allows for in situ SIMPA measurements on interlayer coupling between Fe films as a function d_{Mn} by using one sample only and moving the focused ion beam at the location of the desired d_{Mn} [12]. For further details on the strong influence of d_{Mn} on interlayer couplings, we refer to [12], where it is shown that the Mn interlayer strongly influences surface magnetic domain and domain wall structures. Fig. 3(b) shows the SIMPA spin map of the same surface area obtained after FIB milling. The white, picture-frame shaped area in Fig. 3(b) is created by the removal of the Fe/Mn/Fe films by FIB milling until the surface of the Pd(1 0 0) substrate is reached, which exhibits zero ESP. The grey shades in the images represent different orientations of the in-plane ESP as given by the grey shade wheel in the lower part of Fig. 2. The local orientation and magnitude of the *P* vectors is given by white arrows. It is clearly visible that the overall distribution of the surface magnetization is not changed by the FIB milling, indicating that FIB milling has a negligible
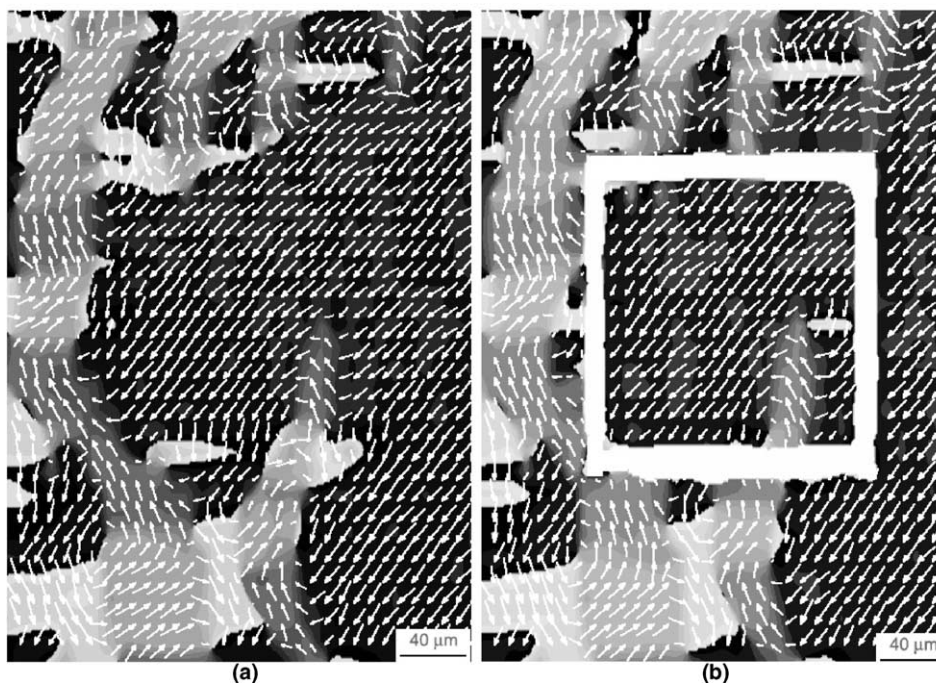

Fig. 2. SIMPA spin map of a circular (35 μm diameter) Co/Si(1 0 0) element, obtained after creating the element by FIB milling and demagnetizing the sample. A grey shade wheel is given in the lower middle part of figure. The grey shades in the image represent the different orientation of the in-plane ESP. The white arrows represent the spatially resolved distribution of the orientation and magnitude of the surface ESP.

Fig. 3. SIMPA spin maps obtained at surfaces of bct Fe(100)/Mn/bct Fe(100)/fcc Pd(100) films for a Mn spacer layer thickness of $d_{Mn} = 4$ ML, where spin map (a) is obtained before FIB milling and spin map (b) is obtained after FIB milling.

effect on the spin-resolved surface magnetic domain and domain wall distribution, and also implying that the interlayer magnetic coupling (MC) [12] between the top and the bottom Fe films in the sandwiched Fe/Mn/Fe/Pd films as well as the magnetic properties of the film system are not changed by the FIB milling.

In conclusion, we have shown that the surface magnetization of FIB created, patterned, 30 nm thick Co elements, is not uniform and that micromagnetic states such as "C" states exist in square-shaped magnetic Co elements and that vortex and anti-vortex states exist in circularly shaped magnetic Co elements. From SIMPA studies at surfaces of tri-layered bct Fe(100)/Mn/bct Fe(100) films deposited on fcc Pd(100) substrates, it is found that FIB milling, which is used to remove magnetic material (Fe/Mn/Fe films) to create patterned elements, has a negligible effect on the surface domain and domain wall distribution at the surface of the topmost Fe film as found by comparing SIMPA spin maps obtained before, during and after FIB milling. The experiments give clear

evidence that SIMPA provides an excellent means to study in situ micromagnetic configurations and to perform in situ FIB milling as well as magnetic sputter depth profiling. The measured SIMPA spin maps, which show the spatial distribution of the orientation and magnitude of the surface magnetization, allow detailed studies of magnetic domains, domain walls and other micromagnetic configurations.

References

[1] G.A. Prinz, Science 282 (1998) 1660;
    G.A. Prinz, J. Magn. Magn. Mater. 200 (1999) 57.
[2] J. Lohau, A. Moser, C.T. Rettner, M.E. Best, B.D. Terris, IEEE Trans. Magn. 37 (2001) 1652.
[3] G. Xiong, D.A. Allwood, M.D. Cooke, R.P. Cowburn, Appl. Phys. Lett. 79 (2001) 3461.
[4] A.Y. Toporov, R.M. Langford, A.K. Petford-Long, Appl. Phys. Lett. 77 (2000) 3063.
[5] W.M. Kaminsky, G.A.C. Jones, N.K. Patel, W.E. Booij, M.G. Blamire, S.M. Gardiner, Y.B. Xu, J.A.C. Bland, Appl. Phys. Lett. 78 (2001) 1589.
[6] J. Li, C. Rau, J. Appl. Phys. 95 (2004) 6527.

[7] C. Chappert et al., Science 280 (1998) 1919.
[8] S.O. Demokritov, C. Bayer, S. Poppe, M. Rickart, J. Fassbeder, B. Hillebrands, D.I. Kholin, N.M. Kreines, O.M. Liedke, Phys. Rev. Lett. 90 (2003) 97201.
[9] Y. Zheng, J.G. Zhu, J. Appl. Phys. 81 (1997) 5471.
[10] J. Shi, S. Tehrani, Y.F. Zheng, J.G. Zhu, Appl. Phys. Lett. 74 (1999) 2525.

[11] N.J. Zheng, C. Rau, Mater. Res. Soc. Symp. Proc. 313 (1993) 723.
[12] J. Li, C. Rau, J. Magn. Magn. Mater., in press.
[13] The OOMMF code is available for public use at <http://math.nist.gov/oommf>.